Tree Physiology 00, 1–14
https://doi.org/10.1093/treephys/tpad019

Research paper

Investigation of the role of TmMYB16/123 and their targets (*TmMTP1/11*) in the tolerance of *Taxus media* to cadmium

Shangguo Feng[1,2], Kailin Hou[1,2], Hongshan Zhang[1,2], Cheng Chen[3], Jiefang Huang[1,2], Qicong Wu[1,2], Zhenhao Zhang[1,2], Yadi Gao[1,2], Xiaomei Wu[1], Huizhong Wang[1,2,4] and Chenjia Shen[1,2,4]

[1]College of Life and Environmental Sciences, Hangzhou Normal University, Hangzhou 311121, China; [2]Zhejiang Provincial Key Laboratory for Genetic Improvement and Quality Control of Medicinal Plants, Hangzhou Normal University, Hangzhou 311121, China; [3]College of Pharmacy, Hangzhou Normal University, Hangzhou 311121, China; [4]Corresponding authors: H. Wang (whz62@163.com); C. Shen shencj@hznu.edu.cn)

Received July 23, 2022; accepted February 13, 2023; handling Editor Zhibin Luo

The toxicity and stress caused by heavy metal contamination has become an important constraint to the growth and flourishing of trees. In particular, species belonging to the genus *Taxus*, which are the only natural source for the anti-tumor medicine paclitaxel, are known to be highly sensitive to environmental changes. To investigate the response of *Taxus* spp. to heavy metal stress, we analyzed the transcriptomic profiles of *Taxus media* trees exposed to cadmium (Cd^{2+}). In total, six putative genes from the metal tolerance protein (MTP) family were identified in *T. media*, including two Cd^{2+} stress inducible *TMP* genes (*TmMTP1*, *TmMTP11* and *Taxus media*). Secondary structure analyses predicted that TmMTP1 and TmMTP11, which are members of the Zn-CDF and Mn-CDF subfamily proteins, respectively, contained six and four classic transmembrane domains, respectively. The introduction of TmMTP1/11 into the *Δycf1* yeast cadmium-sensitive mutant strain showed that TmMTP1/11 might regulate the accumulation of Cd^{2+} to yeast cells. To screen the upstream regulators, partial promoter sequences of the *TmMTP1/11* genes were isolated using the chromosome walking method. Several myeloblastosis (MYB) recognition elements were identified in the promoters of these genes. Furthermore, two Cd^{2+}-induced R2R3-MYB TFs, TmMYB16 and TmMYB123, were identified. Both in vitro and in vivo assays confirmed that TmMTB16/123 play a role in Cd^{2+} tolerance by activating and repressing the expression of *TmMTP1/11* genes. The present study elucidated new regulatory mechanisms underlying the response to Cd stress and can contribute to the breeding of *Taxus* species with high environmental adaptability.

Keywords: cadmium stress, heavy metal stress, metal tolerance protein, *Taxus media*.

Introduction

The influence of heavy metals is a significant environmental problem and has deleterious impacts on the growth and development of plants (Kaur et al. 2021). Most heavy metals, such as cadmium (Cd^{2+}), are non-essential elements that can cause fatal damage to plants, even at trace levels (Salinitro et al. 2021). The accumulation of Cd can exert different physiological and biochemical processes, including chlorosis, a reduction in the photosynthetic rate, accumulation of reactive oxygen species (ROS), destruction of the membrane system and redox imbalance (Sharma and Dietz 2009, Ismael et al. 2019, Aksoy et al. 2021). Being one of the most toxic elements, Cd can influence human health through the food chain (Clemens et al. 2013).

To survive in Cd-contained soils, many plants have developed special molecular mechanisms to avoid the accumulation of this heavy metal and alleviate its toxicity (Singh et al. 2015). Cd accumulation in plant cells induces the production of ROS, including H_2O_2, $O_2^{\cdot-}$, OH and $^1O_2$ (Considine and Foyer 2021). Plants possess both non-enzymatic and enzymatic antioxidant

systems to repair damage caused by ROS. Several enzymes, including catalase (CAT), ascorbate peroxidase, guaiacol peroxidase (POD) and superoxide dismutase (SOD), play key roles in the enzymatic system, while several chemical compounds, including ascorbate, glutathione, anthocyanins and carotenoids, constitute the non-enzymatic system. Both groups are considered to be responsible for the scavenging and elimination of ROS (Kohli et al. 2019). Under Cd exposure, an elevated ROS scavenging efficiency can protect plants against Cd-induced oxidative stresses (Alves et al. 2020).

The regulation of Cd uptake, transport and translocation is another effective strategy to control Cd toxicity in plants (Zhang et al. 2020). Previous studies have reported that different heavy metals share a series of specialized transmembrane (TM) channels (Moulis 2010). Several classic transporter families have been identified in plants, including ATP-binding cassettes, heavy metal ATPases, natural resistance-associated macrophage proteins and metal tolerance proteins (MTPs) (Chauhan et al. 2021, Gronberg et al. 2021, Guo et al. 2022, Haque et al. 2022). The MTP family plays important roles in maintaining the homeostasis of metal ions in plant cells and enhancing the tolerance to heavy metals (Barber-Zucker et al. 2017). Classic MTP family members contain four to six TM domains and a carboxyl cytoplasmic sequence (Montanini et al. 2007). Based on their characteristics, MTP proteins can be grouped into three subfamilies: Zn-CDF, Mn-CDF and Fe/Zn-CDF (Ibuot et al. 2020).

After being initially isolated from *Arabidopsis* (AtMTP1), a number of MTP family members with diverse functions were identified in different plants. For example, NtMTP1a and NtMTP1b, which sequester Zn and Co into vacuoles, were identified in *Nicotiana tabacum* (Shingu et al. 2005). OsMTP1, a homologous protein of AtMTP1, was reported to be responsible for the transport of Zn as well as Co, Fe and Cd (Menguer et al. 2013). In rice, OsMTP11 was identified as an Mn transporter in the Golgi apparatus (Zhang and Liu 2017, Ma et al. 2018). In cucumber, a plasma membrane transporter, known as CsMTP9, was found to be involved in the efflux of Mn^{2+} and Cd^{2+} from root cells to extracellular space (Migocka et al. 2015). In addition, CsMTP6 and CsMTP7 were shown to play important roles in accumulation of Fe^{2+} and Mn^{2+} in mitochondria (Migocka et al. 2018, Migocka et al. 2019). The heterologous expression of the MTP3 from *Brassica napus* in *Arabidopsis* seedlings was found to enhance the tolerance to Zn^{2+} and Mn^{2+} stresses (Gu et al. 2021). More recently, 22 members of the MTP family were identified in the poplar tree (*Populus trichocarpa*) (Gao et al. 2020). MTP6 of poplar serves as an Mn and Co transporter and is essential in the distribution of these two elements (Yang et al. 2021). However, little is known about the MTP family members in the *Taxus* genus.

Taxus plants (also known as yews) are major sources of paclitaxel (trade name: Taxol), a widely used anti-tumor drug (Haddad et al. 2022). The growth and secondary metabolism of *Taxus* trees can be significantly affected by various environmental stressors. For example, leaf traits, gas exchange parameters and the secondary metabolites of *Taxus mairei* were found to undergo significant changes in response to UV-B radiation (Zu et al. 2010). Studies have shown that *Taxus* trees adopt a series of strategies to minimize the damages caused by environmental stresses, including the enhancement of antioxidant systems, and activation of secondary metabolisms and various structural phospholipids (Han et al. 2009, Zheng et al. 2016, Meng et al. 2017). Cadmium pollution is a serious threat to the growth and development of *Taxus* trees; thus, it is crucial to elucidate their molecular responses to Cd exposure. *Taxus* × *media*, a hybrid *Taxus* species with a high content of paclitaxel, is cultivated for the large-scale extraction of Taxol (C. Yu et al. 2017).

Here, we used transcriptomic analysis to reveal the transcriptional responses and tolerance mechanisms of *T. media* seedlings exposed to Cd. Furthermore, two MTP family genes, *TmMTP1* and *TmMTP11*, and their potential regulators, TmMYB16 and TmMYB123, were identified in *T. media*. The results of this study contribute to elucidating the mechanism regulating the response to heavy metal stress and consequently will facilitate the breeding of *Taxus* trees with high environmental adaptability.

Materials and methods

Plant materials and Cd^{2+} treatment

Three-year-old *T. media* trees were grown in a greenhouse at Hangzhou Normal University, Hangzhou, China (120.2E, 30.3N), at a temperature of 26 ± 1 °C, a light cycle of 8/16 h (light/dark) and a relative humidity of 60–70%. For Cd^{2+} treatment, *T. media* trees were planted in two groups of 30 × 30 cm glass pots, three seedlings per group, with a half-strength Hoagland solution. Nutrient solution without cadmium chloride was used for the control group. Nutrient solutions containing 100, 200 and 300 μM of cadmium chloride were used in the treatment groups. Then, plant samples at time point 7 days were harvested and stored at −80 °C to await further analysis.

Biochemical assays

For chlorophyll determination, leaf samples (500 mg) were harvested and ground in a pre-cold mortar with acetone solution. The acetone extract was centrifuged at 2500 × *g* for 10 min, and the supernatant was harvested. Absorbance measurement was performed at 750, 663, 652, 645 and 470 nm by a fluorescence spectrophotometer. The proline contents were determined by a kit that was purchased from Nanjing Jiancheng Bioengineering Institute (http://www.njjcbio.com/) following the manufacturer's instructions. Malondialdehyde concentrations were determined using 2-thiobarbituric acid (TBA) reactions. Leaf samples (200 mg) were homogenized in TBA solution (0.25% TBA in 10% trichloroacetic acid). The extract was

boiled in hot water for 25 min, quickly put on ice until cool and then centrifuged at 5000 × *g* for 10 min. The supernatant was then collected for absorbance measurement at 532 and 600 nm.

The activities of SOD, POD and CAT were determined in accordance with a previous study (Najeeb et al. 2011). Superoxide dismutase activity was measured by the photochemical nitroblue tetrazolium (NBT) assay. In brief, leaves of *T. media* (500 mg) were homogenized with 5 ml of extraction buffer (50 mM phosphate) on ice. Photoreduction of NBT was detected at 560 nm in a working solution (pH 7.8) containing 26 mM L-methionine, 750 μM NBT, 1 μM Ethylene Diamine Tetraacetic Acid (EDTA), 50 mM phosphate and 20 μM riboflavin. For POD determination, guaiacol was added to homogenized leaf samples as a substrate. Then, a reaction mixture solution was added containing 50 mM phosphate buffer solution (PBS) (pH 6.1), 1% guaiacol and 0.4% H_2O_2. The POD extract was collected for absorbance measurement at 470 nm. Catalase activity was estimated in a PBS solution containing 10 mM H_2O_2 and sample extract. The CAT extract was collected for absorbance measurement at 470 nm.

RNA isolation and sequencing

Total ribonucleic acids (RNAs) isolated and sequencing were performed as our previous study (Yu et al. 2021). To obtain quality overview of the transcriptomic responses to Cd treatment, individual RNAs from the control and Cd-treated groups (0 and 7 days after treatment) of three biological replicates were applicated for complementary DNA (cDNA) library construction. The RNA sequencing was carried out on Illumina HiSeq™ 4000 platform (LC-Bio, Hangzhou, China) to produce 100/50-bp paired/single-end small reads.

Pre-processing of transcriptomic datasets

Sequencing adapters, reads with low-quality bases (Q value < 19) and reads with many unknown nucleotides ($N > 5\%$) were filtered out. D*e novo* assembly was performed using the Trinity program to generate unigenes (Grabherr et al. 2011). For unigene annotation, all unigene sequences were aligned by the BLASTX program against several protein databases (Ye et al. 2018). The transcriptomes of *T. media* trees have been uploaded to the NCBI database under accession number GSE175645.

Analysis of DEGs

All clean reads were mapped onto the reference sequence using Bowtie software ver. 0.12.7 to calculate the count of each assembled unigene. Then, the expression level of each unigene was calculated by the reads per kilobase million reads method. Differential expression analysis of unigenes between the control and Cd-treated samples was carried out by the DESeq R package v1.10.1 with a rigorous algorithm method. A corrected false discovery rate ≤ 0.001 and $|\log2 \text{ ratio}| \geq 1$ were set as the threshold to evaluate significance.

QRT-PCR analysis of Cd responsive genes

The expression level of six MTP family genes were further confirmed by the quantitative reverse transcription polymerase chain reaction (qRT-PCR) method. The specific primer sequences are listed in Table S1 available as Supplementary data at *Tree Physiology* Online. The *ACTIN* gene was applied as an internal standard to calculate relative folds by comparative cycle threshold ($2^{-\Delta\Delta Ct}$) values. Three independent cDNA samples from the control and Cd-treated groups were used for the qRT-PCR experiments. The detailed procedure was similar to our previous work (Chunna et al. 2017).

Cloning of CDS and promoter sequences

Partial sequences of the *TmMTP1*, *TmMTP11*, *TmMYB16*, and *TmMYB123* genes were obtained from the transcriptomes. Taking the partial sequences as templates, the full-length sequences of these genes were amplified using a SMARTer RACE 5′/3′ Kit (Clontech, Dalian, China). In brief, a mixture solution containing 1 μg of total RNA from young leaves, 1 μl of 5′ or 3′ primers, 1 μl of SMARTer II oligonucleotide A and ddH_2O was prepared as the RACE working solution. Then, 4 μl of 5 × First Strand buffer, 0.5 μl of 100 mM dithiothreitol, 1 μl of 20 mM dNTP mix, 20 U of RNase inhibitor and 200 U of SMARTScribe Reverse Transcriptase were added to the RACE working solution. The upstream promoter regions of *TmMTP1* and *TmMTP11* genes were amplified using a Clontech Genome Walker Kit (Dalian, China). The primers used for RACE are listed in Table S1 available as Supplementary data at *Tree Physiology* Online.

Basic bioinformatics analysis

The full-length sequences of *TmMTP1* and *TmMTP11* were cloned into the pCAMBIA1300-35S vector. The primers used for subcellular localization experiments are listed in Table S1 available as Supplementary data at *Tree Physiology* Online. The empty pCAMBIA1300 vector was used as a negative control. Constructs were transferred into *Agrobacterium tumefaciens* (GV3101 stain) cells and transiently expressed in *Nicotiana tabacum* epidermal cells. The Green fluorescent protein (GFP) emitted by the target proteins was detected using a Carl Zeiss LSM710 confocal microscope.

Unrooted phylogenetic tree was built using MEGA software ver. 7.1 and CLUSTALW program employing the Neighbor-Joining (NJ) method.

The physical and chemical properties of TmMTP1 and TmMTP11 were online analyzed using ExPASy ProtParam (https://wed.expasy.org/protparam). The transmembranehelices (TMH) domain of TmMTP proteins was analyzed using the TMHMM online tool (https://services.healthtech.dtu.dk/servi

ce.php?TMHMM-2.0). The *cis*-acting elements of TmMTP promoters were predicted using PlantCARE software (http://bioinformatics.psb.ugent.be/webtools/plantcare/html/).

Method of yeast complementation

Wild-type yeast BY4741 (*MATα*; *his3Δ1*; *leu2Δ0*; *met15Δ0*; *ura3Δ0*) and mutant yeast *Δycf1* (*MATα*; *his3Δ1*; *leu2Δ0*; *met15Δ0*; *ura3Δ0*; *YDR135c*; WI, *kanMX4*) were used in this experiment. The sequences of *TmMTP1* and *TmMTP11* were inserted into the pYES2 vector and ectopically expressed in the two yeast stains. The transformed cells were cultured in liquid nutrient medium (SD-U) containing glucose. When the OD_{600} reached 0.7–0.8, the solution was serially diluted (OD_{600}: 0, 10^{-1}, 10^{-2}, 10^{-3} and 10^{-4}). The resulting cells were then placed on a galactose solid medium (SG-U) containing 0, 10 and 20 μM Cd and then incubated at 30 °C for 3 days. Yeast were cultured in SG-U medium to an OD_{600} of 0.25. Then, 20 μM Cd was added to the medium and the OD_{600} values were determined every 5 h to record growth curves (Li et al. 2021).

Determination of Cd^{2+} content

The yeast cells were harvested, washed five times with double distilled H_2O and dried at 85 °C for 2 days. Then, the cells were treated with 5 ml of nitric acid. The metal concentration is measured by Inductively Coupled Plasma Optical Emission Spectrometry (ICP-OES) (ICP-OES-7000, Thermo Fisher Scientific, New York, NY, USA).

Prokaryotic expression and EMSA

The full-length sequences of *TmMYB16* and *TmMYB123* genes were inserted into vector pGEX-4 T with multiple cloning sites BamHI/SalI and transformed into *Escherichia coli* cells to produce artificial His-tag recombinant protein. Primers for prokaryotic expression are listed in Table S1 available as Supplementary data at *Tree Physiology* Online. Then, Isopropyl-β-D-thiogalactopyranoside (IPTG) (1 mM) was used to induce protein accumulation at 30 °C for 3 h. The resulting proteins were extracted and tag-purified using Clontech His60-Ni-Resin according to its methods.

Electrophoretic mobility shift assay (EMSA) was performed as our previous published work (Yu et al. 2020). Briefly, sequences containing MYB-binding element (MBE) (core elements: CAGTTA or TGGTTA) derived from the promoter sequences of *TmMTP1* and *TmMTP11* were labeled with the 5(6)-FAM dye to produce probes. Sequences without a fluorescent dye were used as competition probes. The core sequence in probe was changed to CCCGGG and used as mutation probes. All probes used in EMSA are listed in Table S1 available as Supplementary data at *Tree Physiology* Online.

Dual-luciferase reporter assay

The coding sequences (CDSs) of *TmMYB16* and *TmMYB123* were cloned into the pBD-35S vector as effectors. The promoters of *TmMTP1* and *TmMTP11* were inserted into the pGreenII-0800-LUC vector as double-reporters. The Luciferase (LUC) and Renilla (REN) luciferase activities were determined using a dual-luciferase assay kit (Promega, Madison, USA) according to its instruction. The binding activities of TmMYB16 and TmMYB123 to *TmMTP1* and *TmMTP11* promoters were determined by the LUC/REN ratios. Primers for the dual-luciferase assay are listed in Table S1 available as Supplementary data at *Tree Physiology* Online.

Statistical methods

A one-way analysis of variance was applied to compare data, including biochemical measurements, functional analysis in yeasts and LUC activity, between the control and Cd^{2+} treatment groups. For the biochemical measurement, yeast complementation and dual-LUC assays, three biological replicates were used. For transcriptomic analysis, *P*-values were calculated by false discovery rate (FDR) analysis and adjusted by the Benjamini–Hochberg method. False discovery rate analysis was applied to screen differentially expressed genes (DEGs) between the control and Cd^{2+} treatment groups. *P*-value < 0.05 was considered to be statistically significant.

The statistical calculation was performed using SPSS software ver.19.0.

Results

Physiological responses of T. media seedlings to Cd stress

To investigate the physiological changes in *T. media* seedlings under different Cd treatments, several important physiological parameters and antioxidant enzymatic activities were determined. The chlorophyll contents were significantly reduced under 100 and 200 μM Cd^{2+} treatments (Figure 1a). Proline content was significantly upregulated under exposure to 200 and 300 μM Cd^{2+} (Figure 1b). Malondialdehyde content significantly increased under different Cd concentrations (Figure 1c). The activities of SOD were downregulated and reached the lowest level under exposure to a Cd^{2+} concentration of 200 μM (Figure 1d). Catalase activity was also downregulated (Figure 1e), while POD activity was upregulated and reached the highest level at a Cd^{2+} concentration of 300 μM (Figure 1f).

Transcriptome of T. media under Cd stress

RNA sequencing was performed to reveal the transcriptional responses of *T. media* seedlings to Cd stress. A total of 39.52 Gb of sequence data were acquired, consisting of 18.68 Gb from the control group and 20.84 Gb from the Cd-treated group (Table S2 available as Supplementary data at *Tree Physiology* Online). After filtering, clean reads produced 117,536 transcripts (N50: 1730), with a mean length of 637 bp, and 67,056 unigenes (N50: 1606), with a mean length of 457 bp (Figure S1 available as Supplementary data at *Tree Physiology* Online).

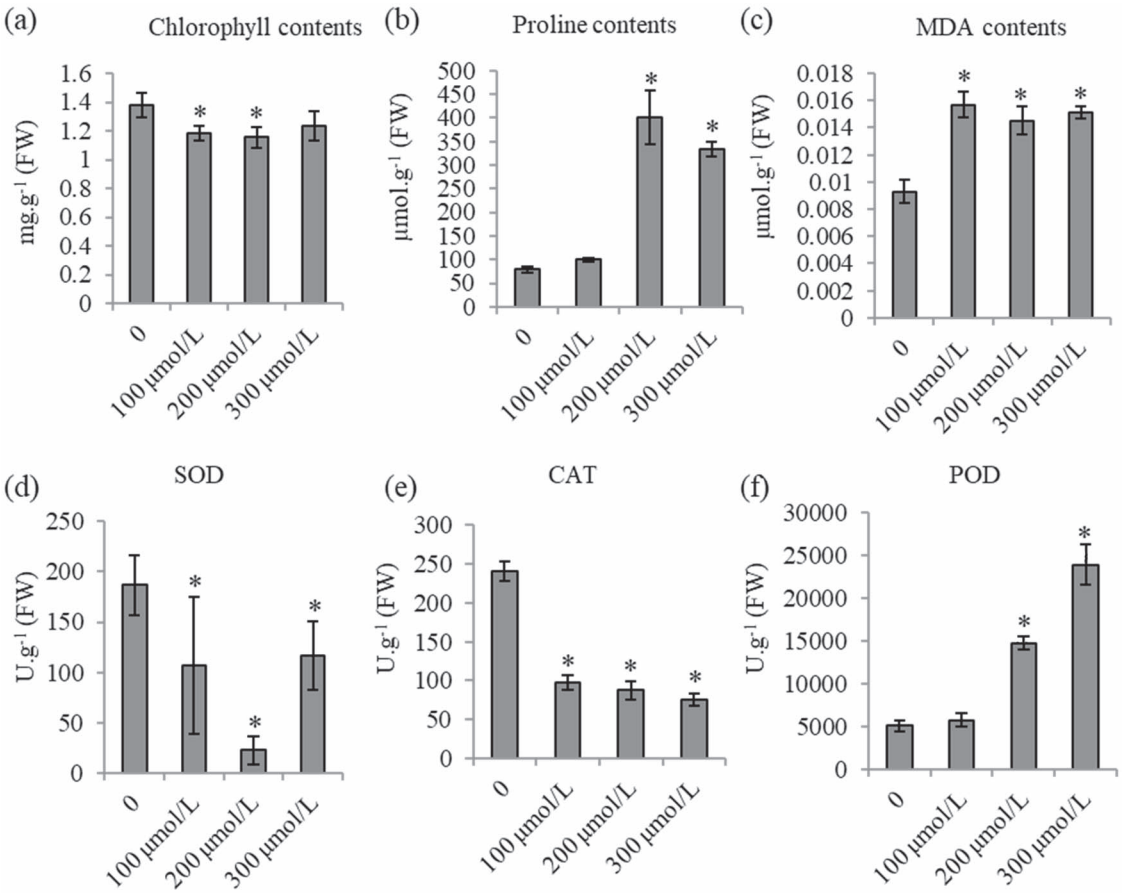

Figure 1. Physiological responses of *T. media* seedling to Cd stress. Cadmium induced changes in chlorophyll contents (a), proline contents (b) and malondialdehyde contents (c). The activities of key antioxidant enzymes, such as SOD (d), CAT (e) and POD (f), under Cd treatment. '*' indicates significant differences between control and Cd treatment at $P < 0.01$. Three biological replicates were performed in each comparison group.

In terms of regards to size distribution, 14.42% of the transcripts and 11.31% of the unigenes were more than 2000 bp in length (Figure S2a available as Supplementary data at *Tree Physiology* Online). In total, 67,056 of the unigenes were annotated using several databases: 29,687 unigenes in Gene Ontology (GO), 18,748 unigenes in the Kyoto Encyclopedia of Genes and Genomes (KEGG), 25,629 unigenes in Pfam, 27,052 unigenes in SwissProt and 317,796 unigenes in eggNOG (Figure S2b available as Supplementary data at *Tree Physiology* Online). The protein similarity analysis suggested that the majority of predicted proteins in *T. media* were highly similar to the proteins in *Picea sitchensis*, *Amborella trichopoda* and *Nelumbo nucifera* (Figure S2c available as Supplementary data at *Tree Physiology* Online). Most unigenes were classified into various KEGG metabolic and signaling pathways, such as 'carbohydrate metabolism' (1364 unigenes), 'translation' (1151 unigenes) and 'folding, sorting and degradation' (1109 unigenes) (Figure S2d available as Supplementary data at *Tree Physiology* Online).

Identification of DEGs responsive to Cd stress

Under Cd exposure, 826 DEGs, including 687 increased and 139 decreased genes, were obtained (Figure 2a and b). A total of 650 DEGs were categorized into at least one GO term (Figure S3 available as Supplementary data at *Tree Physiology* Online). Subsequently, the DEGs were mapped onto canonical reference KEGG pathways to analyze the differential metabolic pathways under Cd treatment. The most significant KEGG terms were 'ribosome' (66 DEGs), 'oxidative phosphorylation' (16 DEGs) and the 'mitogen-activated protein kinase (MAPK) signaling pathway' (16 DEGs) (Figure S4 available as Supplementary data at *Tree Physiology* Online).

Several metal ion GO terms associated with stress responses were identified. The most enriched GO terms related to metal ion were 'cellular transition metal ion homeostasis' ($P = 0.085$) and 'transition metal ion binding' ($P = 0.005$). The most enriched GO terms related to the oxidation–reduction process were 'antioxidant activity' ($P = 2.56E{-}12$), 'oxidoreductase activity' ($P = 2.43E{-}12$), 'oxidation–reduction process' ($P = 4.86E{-}07$) and 'response to oxidative stress' ($P = 5.79E{-}08$) (Figure 2c). For the following terms, a number of upregulated and downregulated genes were observed (reported respectively in parentheses): 'antioxidant activity' (9 and 3), 'transition metal ion binding' (4 and 1), 'oxidation–reduction process' term (58 and 2) and 'cellular transition metal ion homeostasis' (2 and 1). In contrast, for

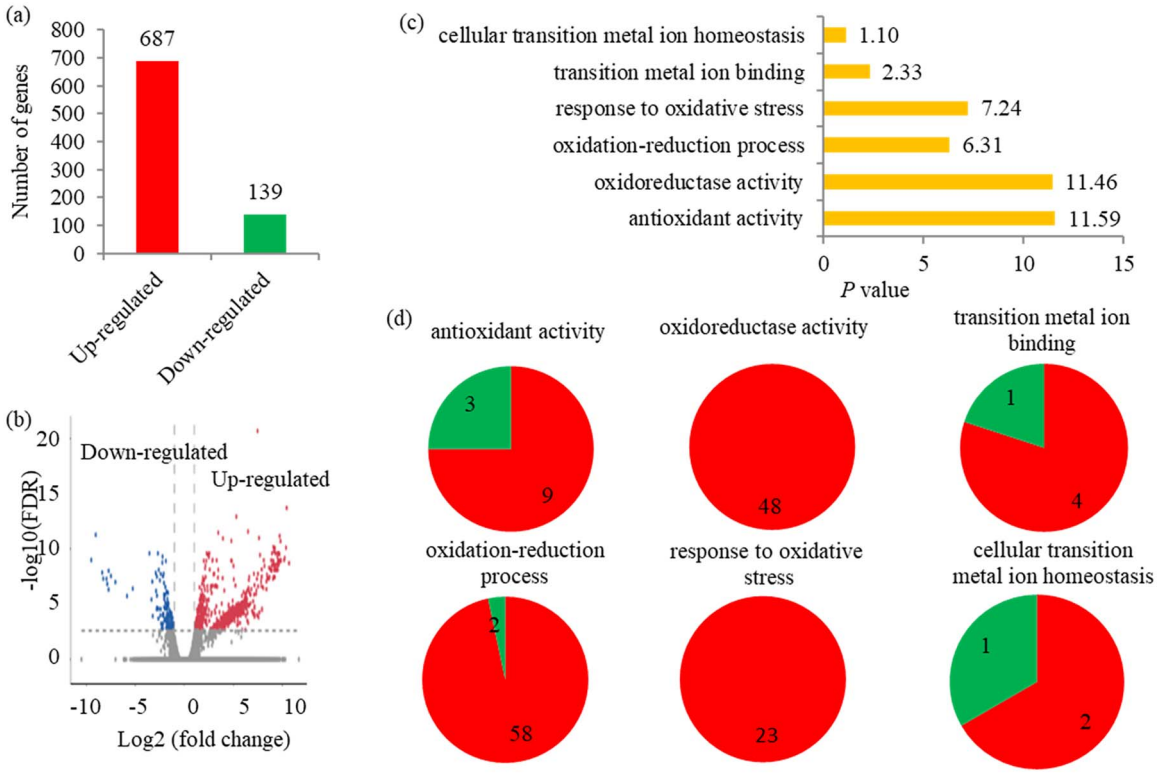

Figure 2. Analysis of differential expressed genes of *T. media* under Cd treatment. (a) Numbers of the up- and down-regulated genes of *T. media* under Cd treatment. (b) Volcano plots of the DEGs under Cd treatment. (c) Enrichment analysis of metal ion-related GO terms. (d) Numbers of the increased and decreased genes in each metal ion-related GO term.

the 'oxidoreductase activity' and 'response to oxidative stress' terms, no downregulated genes were observed (Figure 2d).

Cloning and basic analysis of the MTP family

Based on the transcriptome, six putative *MTP* family genes were identified in *T. media*. The CDSs of the six *MTP* family genes were cloned (Dataset S1 available as Supplementary data at *Tree Physiology* Online). Evolutionary analysis showed that all putative MTP members were grouped into three different subgroups: Zn-CDF (TmMTP1 and TmMTP5), Fe/Zn-CDF (TmMTP6 and TmMTP7) and Mn-CDF (TmMTP8 and TmMTP11) (Figure 3a). Quantitative real-time PCR was performed to confirm the changes in expression of the *TmMTP* family genes under Cd exposure. The results showed that *TmMTP1* and *TmMTP11* were significantly upregulated (Figure 3b); hence, we focused on these two genes in subsequent analyses.

To examine their subcellular localization, the eGFP-tagged TmMTP1 and TmMTP11 fusion proteins were heterologously expressed in tobacco leaves. Our data showed that the two proteins were localized on the cell membrane, which is consistent with the prediction that TmMTP1/11 are transporters (Figure S5 available as Supplementary data at *Tree Physiology* Online). Six TMHs were identified in TmMTP1 protein, including four HMs at the N-terminus and two HMs at the C-terminus, while four HMs were detected in the middle of TmMTP11 (Figure 3c). Multiple sequence alignment confirmed that both proteins possessed classic TM domains (Figure 3d–e).

Yeast complementation analysis of TmMTP1/11 proteins

The *Saccharomyces cerevisiae* strain ycf1 is a Cd-sensitive strain resulting from the deletion of the *yeast cadmium factor 1* (*YCF1*) gene, which is a glutathione S-conjugate pump located on the vacuolar membrane (Li et al. 1997). Yeast cadmium factor 1 transports Cd-GS2 and glutathione-S-conjugates from the cytosol into the vacuole and confers *S. cerevisiae* cells resistance to Cd, As, Sb, Hg and Pb (Gueldry et al. 2003). To investigate the cellular function of *TmMTP1* and *TmMTP11*, the two genes were ectopically expressed in wild-type (BY4741) and mutant (*Δycf1*) yeast cells. When exposed to 25 μM Cd, the growth rate of *Δycf1* cells was significantly higher than that of the wild type. The growth rate of *Δycf1* cells carrying pYES2-*TmMTP1/11* was obviously higher than that of *Δycf1* cells carrying the empty pYES2 plasmid (Figure 4a). To investigate the function of TmMTP1 and TmMTP11, the content of Cd was determined in the different yeast cell lines. The results showed that the content of Cd in *Δycf1* cells was significantly lower than in BY4741. *Δycf1* cells carrying *TmMTP1* or *TmMTP11* had a significantly higher content of Cd compared with *Δycf1* cells carrying the empty vector, suggesting that TmMTP1/11 might be involved in the accumulation of Cd in yeast cells (Figure 4b).

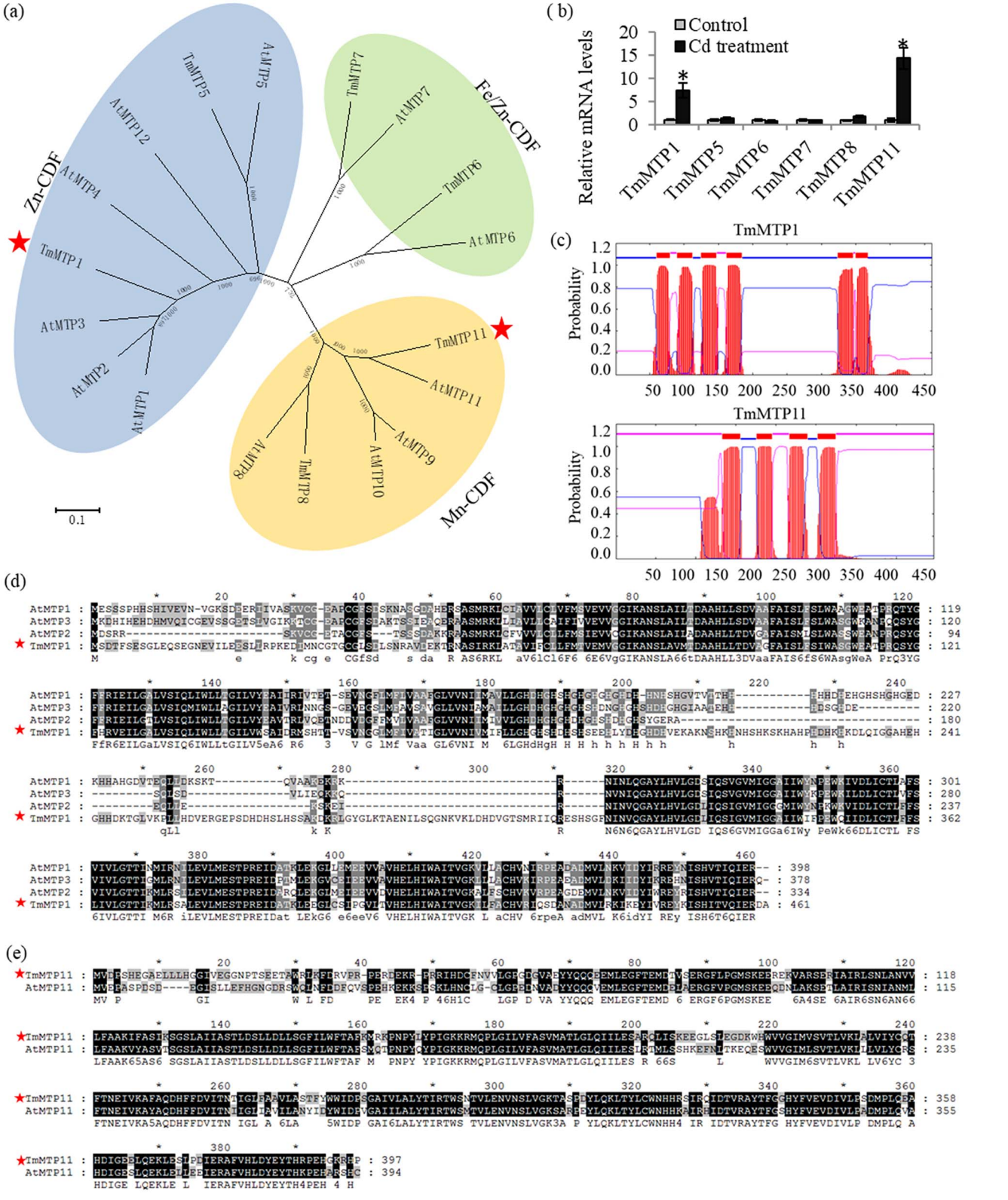

Figure 3. Identification and analysis of *T. media* MTP proteins. (a) Evolutionary analysis of MTP proteins from *T. media* and *Arabidopsis*. Stars indicated TPM proteins from *T. media*. Phylogenetic tree was built using MEGA software ver. 7.1 and CLUSTALW program employing the NJ method. (b) Expression analysis of *T. media* MTP family genes under Cd treatment. "∗" indicated significantly differences ($P < 0.05$) in gene expression between control and Cd treatment groups. (c) Predication of transmembrane domains in TmMTP1 and TmMTP11. (d) Sequence alignment of TmMTP1 and MTP1/2/3 in Arabidopsis. (e) Sequence alignment of TmMTP11 and MTP11 in *Arabidopsis*. Conserved residues are shown in deep background.

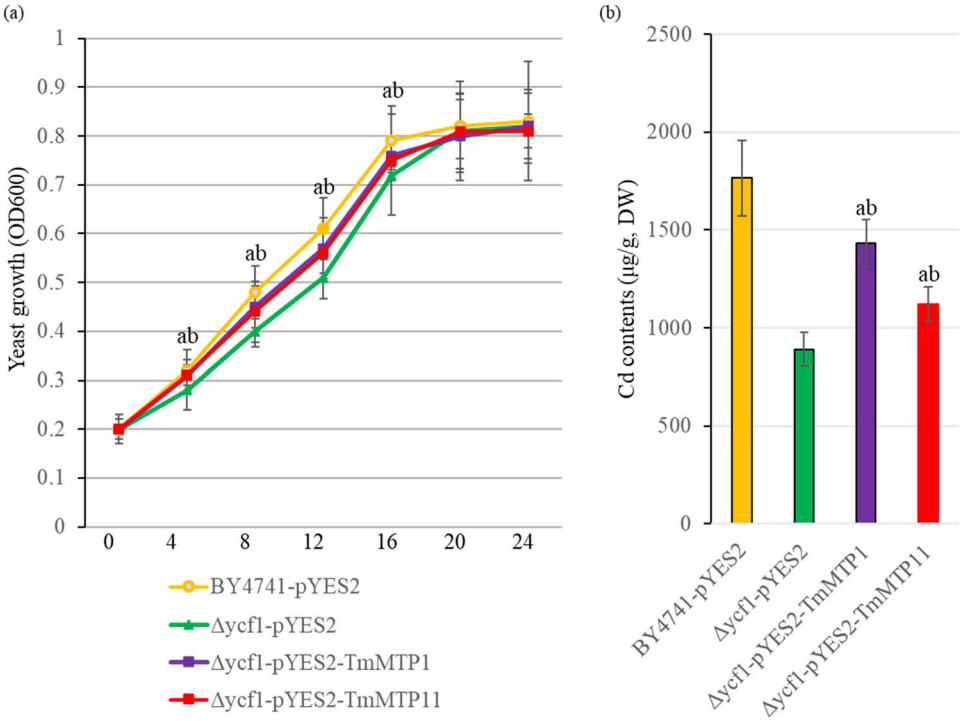

Figure 4. Functional analysis of TmMTP1 and TmMTP11. (a) The status of yeast cells at different time points during the growth process. The OD_{600} of yeast cells was cultured to 0.2, $CdCl_2$ was added to make the medium concentration reach 25 μM, then samples were measured every 4 h. (b) The Cd contents in different yeast cells. Letter 'a' indicates significant differences between control (BY4741-pYES2) and treatment groups at $P < 0.01$. Letter 'b' indicates significant differences between control (*Δycf1*-pYES2) and treatment groups at $P < 0.01$. Three biological replicates were performed in each comparison group.

Isolation and analysis of the promoters of TmMTP1 and TmMTP11

Promoter sequences contain abundant genetic information. Due to the lack of a genome sequence for *T. media*, partial promoter sequences for *TmMTP1* and *TmMTP11* were cloned and used to scan *cis*-elements. The results revealed one MBE in the promoter region of *TmMTP1* and four MBEs in the promoter region of *TmMTP11* (Figures S6 and S7 available as Supplementary data at *Tree Physiology* Online). Thus, we focused on the function of MYB family genes in the transcriptional regulation of *TmMTP1/11* in subsequent analyses.

Cloning and basic analysis of MYB family genes responsive to Cd stress

Based on the assembled transcriptomic sequence, a total of 50 MYB family members were identified (Table S3 available as Supplementary data at *Tree Physiology* Online). Expression analysis identified two Cd stress-responsive MYB genes: *TmMYB16* and *TmMYB123*. Their partial core sequences were extracted from the assembled reference sequence as specific templates. Then, the full-length CDSs of *TmMYB16* and *TmMYB123* genes were amplified. Phylogenetic analysis showed high similarities between TmMYB16/GbMYB16 and TmMYB123/AtMYB123 (Figure 5a). Multiple sequence alignment further revealed that TmMYB16 and TmMYB123 possess typical R2R3 domains at the N-terminus. No classic repressors, such as EAR and Three L repression (TLLLFR) motifs, were found at the C-terminus of the TmMYB16 and TmMYB123 proteins (Figure 5b).

Sequence analysis further indicated that *TmMYB16* and *TmMYB123* encode putative proteins with 1176 and 753 amino acid residues, respectively. To investigate their downstream target genes, prokaryotic expression and affinity purification of the Glutathione S-transferase (GST)-TmMYB16 and -TmMYB123 proteins were performed (Figure 5c).

TmMYB16/123 enhanced the expression of TmMTP1 and TmMTP11

To investigate the roles of TmMYB16/123 in heavy metal tolerance, the binding of TmMYB16/123 to their potential target promoters was analyzed. Several probes surrounding the MBEs in the promoter regions of *TmMTP1* (P1: −1066 ∼ −1060) and *TmMTP11* (P1: −1427 ∼ −1421; P2: −1278 ∼ −1272; P3: −1152 ∼ −1146; and P4: −791 ∼ −785) were prepared for EMSA assays (Figure 6a). The results showed that neither TmMYB16 or TmMYB123 could bind to the P1, P3 and P4 regions in the *TmMTP11* promoter. TmMYB16/123 bound directly to P1 and P2 in the *TmMTP1* and *TmMTP11* promoters, respectively. Application of excess cold competitive probes significantly reduced the binding of TmMYB16/123 proteins to the positive probes while mutated probes did not affect binding activities (Figure 6b–e).

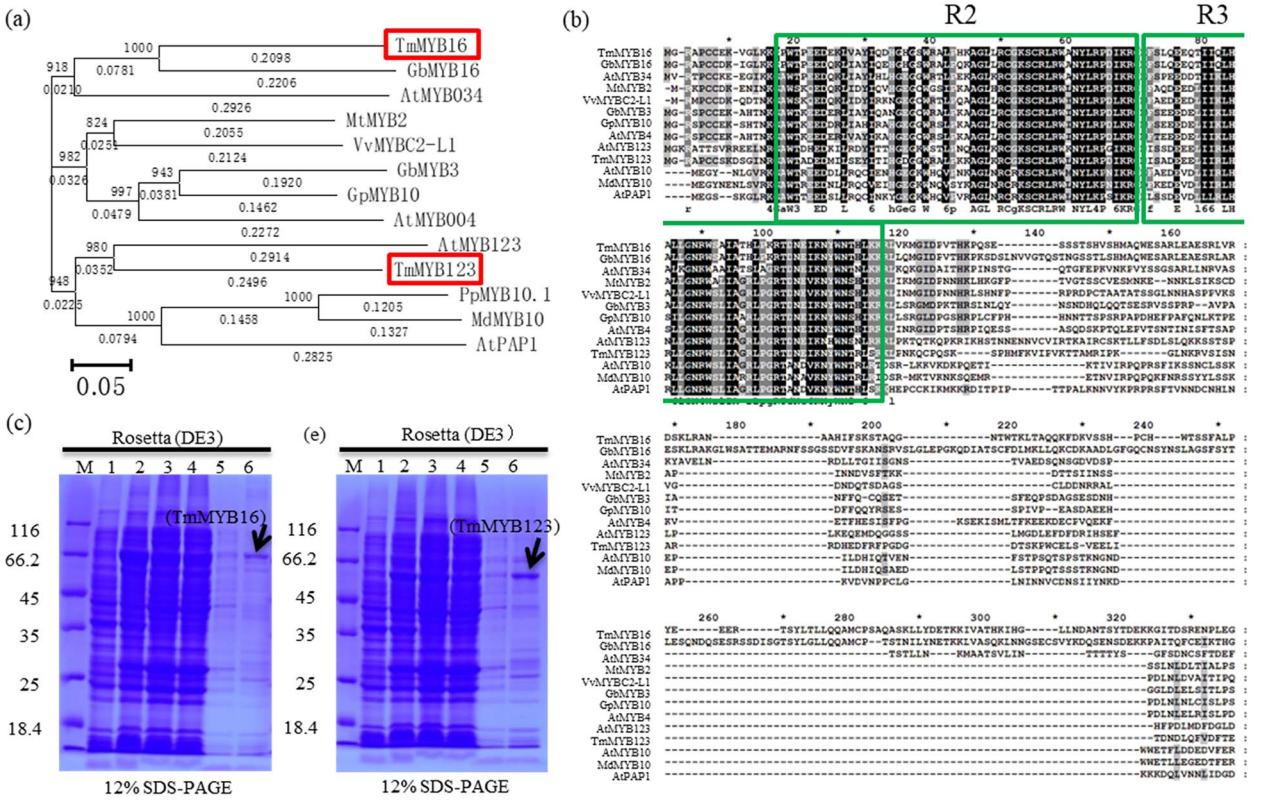

Figure 5. Identification and analysis of *T. media* MYB factors. (a) Evolutionary analysis of MYB factors from *T. media* and other plants. Phylogenetic tree was built using MEGA software ver. 7.1 and CLUSTALW program employing the NJ method. (b) Sequence alignment of TmMYB16/123 and several known R2R3-MYB TFs from other plants. Conserved residues are shown in deep background. The R2 and R3 repeats are indicated with boxes. (c) Prokaryotic expression of TmMYB4 and TmMYB34 in Escherichia coli cells. M: Protein Marker 26610; Line 1: total cell lysate (un-induction); Line 2: total cell lysate (after induction) Line 3: loading solution; Line 4: effluent solution; Line 5: 10 mMGSH eluent; and Line 6: 50 mM GSH eluent.

To analyze the transcriptional activities of TmMYB16/123, we performed dual-luciferase reporter assays in tobacco leaf samples. The full-length CDSs of *TmMYB16* and *TmMYB123*, and the cloned promoter sequences from the *TmMTP1* and *TmMTP11* genes, were used to construct vectors (Figure 7a). Our data showed that TmMYB16 repressed the expression levels of *TmMTP1* and *TmMTP11*, indicating that TmMYB16 functions as a transcriptional repressor (Figure 7b). In contrast, TmMYB123 significantly upregulated the expression of *TmMTP1* and *TmMTP11*, thus suggesting that it acts as a transcriptional activator (Figure 7c).

Discussion

As well-known gymnosperms with a high ornamental and medicinal value, *Taxus* trees have been widely studied in terms of their response to environmental stressors, such as acid rain stress, UV-B radiation and elevated levels of O_3 (H. Yu et al. 2017, Hu et al. 2022, Jiao et al. 2022). Cd^{2+} is one of the most widespread heavy metal ions posing environmental health-related risks to plants (Ismael et al. 2019). Elucidating the key TFs that are responsive to Cd stress could assist in developing a potential model to explain the response of *Taxus* trees to other environmental stresses.

Transcriptomic analysis is an effective tool that can reveal the genes of *Taxus* plants responsive to environmental stressors. In the present study, a total of 67,057 unigenes were identified in *T. media*, suggesting that our transcriptome had a reasonable sequencing depth. Several transcriptomic studies conducted on the *Taxus* genus revealed 3643 DEGs (6.9% of all detected genes) responsive to UV-B radiation, and 2025 DEGs (3.2% of all detected genes) responsive to cold stress (Meng et al. 2017, Jiao et al. 2022). In *T. media*, only 826 genes (1.2% of all detected genes) were identified as DEGs under Cd exposure, suggesting that the response of *Taxus* tree to Cd stress was weaker than those to UV-B and thermal stressors.

The classic MTP family consists of three major clusters based on their transported substrate specificities, including Zn-CDF, Fe/Zn-CDF and Mn-CDF (Montanini et al. 2007). Previous evolutionary analyses grouped TmMTP1 and six AtMTPs (AtMTP1-5 and AtMTP12) into the Zn-CDF subfamily, suggesting that TmMTP1 is a potential Zn^{2+} transporter (Gustin et al. 2011). Moreover, TmMTP11 and four AtMTPs (AtMTP8-11) were grouped into the Zn-CDF subfamily, suggesting

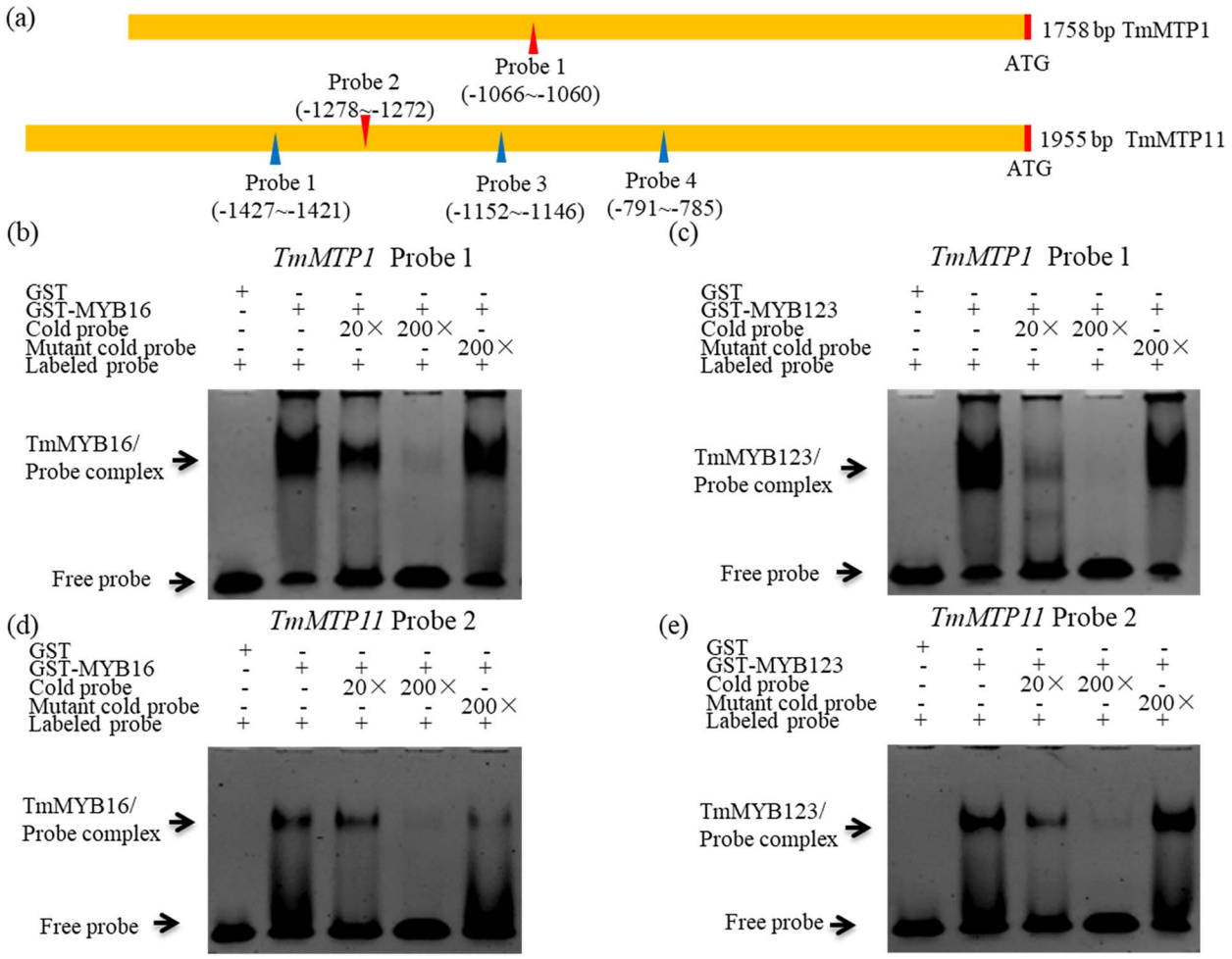

Figure 6. EMSA analysis of the binding of TmMYBs to the promoters of *TmMTP1* and *TmMTP11* genes. (a) The locations of MBEs in the promoter regions of *TmMTP1* and *TmMTP11* genes. Arrows indicate the MBEs. The GST only or TmMYB16-GST fusion proteins were incubated with probes containing the MBEs derived from the promoters of *TmMTP1* (b) and *TmMTP11* (c). The GST only or TmMYB123-His fusion proteins were incubated with probes containing the MBEs derived from the promoter sequences of *TmMTP1* (d) and *TmMTP11* (e). '+' and '−' represent presence and absence, respectively, and 20× and 200× show increasing amounts of probes.

that TmMTP11 is a potential Mn^{2+} transporter. In plants, the substrates of MTP are not unique. For example, cucumber's MTP6 was shown to be involved in mitochondrial Fe^{2+} and Mn^{2+} homeostasis (Migocka et al. 2019), while *Populus trichocarpa*'s MTP6 was shown to transport Co^{2+}, Fe^{2+} and Mn^{2+} (Gao et al. 2020).

The phylogenetic tree displayed that TmMTP1 showed close similarity to AtMTP1/2/3 and TmMTP11 showed close similarity to AtMTP11. In *Arabidopsis*, MTP1/3 were reported to be Zn vacuolar transporters and MTP11 was identified as vacuolar compartment-localized protein (Arrivault et al. 2006, Delhaize et al. 2007). In plants, Cd^{2+} and Zn^{2+} are considered to share transporters (Clemens 2006). The high similarity of protein sequences suggests that TmMTP1/11 are conserved and play an essential role in Cd^{2+} transport. In the present study, heterologous expression in yeast showed that TmMTP1/11 can improve the tolerance of yeast mutant *Δycf1* to Cd^{2+} stress. Also, the expression of TmMTP1/11 significantly increased the Cd concentration in Δycf1 cells. Together, these data strongly suggest that TmMTP1 and TmMTP11 play a role in Cd^{2+} detoxification via sequestration into the vacuole.

Although the genomes of three *Taxus* species, including *T. yunnanensis*, *T. mairei* and *T. wallichiana*, have been recently published (in 2021), the *T. media* genome is still unavailable (Cheng et al. 2021, Song et al. 2021, Xiong et al. 2021). In our study, partial *TmMTP1/11* promoter sequences were cloned using genome walking technology. Recently, several MTP promoters were cloned in various plants (Eroglu et al. 2017, Zhang and Liu 2017). In addition to TATA-box, CAAT-box, TGACG-element and GT1-motif, MBEs were identified in the tobacco *MTP* promoter and *Canavalia rosea* MTP promoters (Papierniak-Wygladala et al. 2020, Zou et al. 2021). Previous data suggested the important roles of MYB family members in heavy metal tolerance. For example, MYB4 and MYB59 in

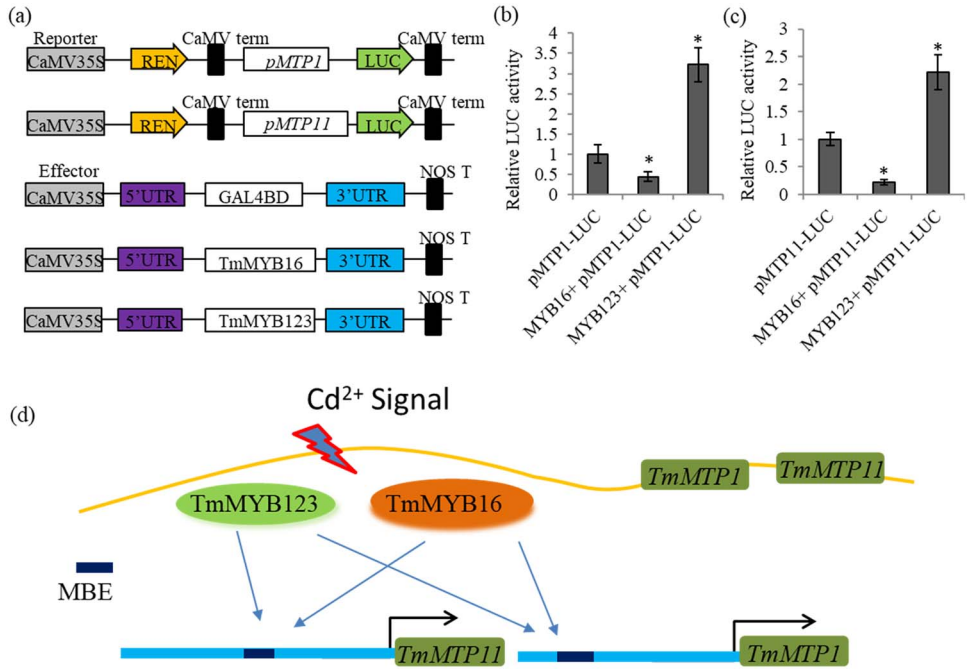

Figure 7. Transcriptional ability of TmMYBs. (a) The detailed information of the transient expression constructs with dual REN/LUC reporters and effectors. CPMV, cowpea mosaic virus; LUC, firefly luciferase; REN, Renilla luciferase; UTR, untranslated regions. (b) The transcriptional abilities of TmMYB16/123 are indicated by the LUC/REN ratios. The pBD vector that produced the GAL4 DNA-BD alone was treated as negative control. Three biological repeats were used in the present study. The asterisks '*' represent significant differences between control and test groups ($P < 0.05$). Three biological replicates were performed in each comparison group. (c) A model for the regulatory roles of TmMYB16/123 is responsive to Cd stress. TmMYB16/123 has a significant effect on responses to Cd stress by activating the expression of *TmMTP1* and *TmMTP11*. (d) A predicted mode of transcription regulation involved in Cd stress responses.

Arabidopsis, MYB2 in ramie, and four MYB-like proteins in barley, have been reported to be specifically involved in Cd^{2+} tolerance (Agarwal et al. 2020, Gao et al. 2020, Zhu et al. 2020, Su et al. 2022). Our transcriptomes identified six MTP family members, including two Cd stress-induced MYB members, providing Cd tolerance-related candidate genes.

Recent researches have focused on the TFs involved in the regulation of taxol biosynthesis (Yu et al. 2020, 2022). So far, few stress-associated TFs have been functionally identified in *Taxus* trees. In *T. media*, two Cd-inducible R2R3-MYB TFs, TmMYB16 and TmMYB123, were identified as potential stress-associated regulators. The closest homologous gene of *TmMYB16* is *GbMYB16*, a MIXTA-like transcription factor (TF) involved in trichome development and epidermal cell differentiation in Ginkgo (Liu et al. 2017). The closest homologous gene of *TmMYB123* is *AtMYB123*, a key determinant in the accumulation of proanthocyanidin in *Arabidopsis* (Heppel et al. 2013). Different downstream target genes were shown to determine to the functional diversity of homologous MYB genes in various plants.

To date, several stress-related functional genes have been reported to be the downstream targets of MYBs. Under Cd exposure, the overexpression of AtMYB4 was shown to enhance the transcript abundance of the *phytochelatin synthase 1* and *metallothionein 1C* genes, suggesting the anti-oxidant defense system is a potential target of MYB TFs (Agarwal et al. 2020). AtMYB47 was shown to enhance Cd accumulation by positively regulating the expression of two isoprenylated genes associated with heavy metals and encoding plant proteins, *HIPP22* and *HIPP44*, suggesting that the chelating system is another potential target of MYB TFs (Zhang et al. 2019). In our study, in vitro and in vivo assays investigated the transcriptional activation of TmMYB123 and repression of TmMYB16 against the promoters of *TmMTP1/11* (Figure 7c). Our data suggested that the heavy metal transport system is also a potential target of MYB TFs.

In conclusion, we acquired the transcriptome profiles of *T. media* under control and Cd exposure conditions. Expression analysis identified two Cd stress-inducible MTP genes, *TmMTP1* belonging to the Zn-CDF cluster and *TmMTP11* belonging to the Mn-CDF cluster. Heterologous expression of *TmMTP1* and *TmMTP11* in yeast increased the tolerance of *Δycf1* cells to Cd^{2+} by sequestration into the vacuole. Furthermore, two Cd stress-induced MYB family genes, *TmMYB16* and *TmMYB123*, were identified. TmMYB16/123 are involved in Cd tolerance by regulating the expression of the *TmMTP1/11* genes. Our data uncovered the regulatory mechanism underlying Cd stress and will facilitate the breeding of *Taxus* species with high environmental adaptability.

Supplementary data

Supplementary data for this article are available at *Tree Physiology* Online.

Data availability

The datasets generated and/or analyzed during the current study are available in the NCBI repository under accession number GSE175645.

Acknowledgments

We are also grateful to LC Sciences company (Hangzhou, China) for transcriptomic analysis.

Conflict of interest

The authors have no relevant financial or non-financial interests to disclose.

Funding

This work was funded by the National Natural Science Foundation of China (32271905); the Zhejiang Provincial Natural Science Foundation of China under Grant Nos. LY23C160001, LY18C050005, LY19C150005, LY19C160001; the Open Foundation of State Key Laboratory of Subtropical Silviculture, Zhejiang A & F University (KF201708); Major Increase or Decrease Program in The Central Finance Level (Grant No. 2060302); and Zhejiang Provincial key Research & Development Project Grants (2017C02011, 2018C02030).

Authors' contributions

S.F., H.W. and C.S. contributed to the study conception and design. Material preparation was performed by S.F., H.K. and H.Z.; data collection was performed by S.F., C.C., J.H. and Q.W.; data analysis was performed by Q.W. and Z.Z.; plants were watered by Y.G.; and RNA sequencing was performed by X.W.. The first draft of the manuscript was written by H.W. and C.S., and all authors commented on the previous versions of the manuscript. All authors read and approved the final manuscript.

References

Agarwal P, Mitra M, Banerjee S, Roy S (2020) MYB4 transcription factor, a member of R2R3-subfamily of MYB domain protein, regulates cadmium tolerance via enhanced protection against oxidative damage and increases expression of PCS1 and MT1C in Arabidopsis. Plant Sci 297:110501.

Aksoy E, Uncu AT, Filiz E, Orman S, Cetin D, Akbudak MA (2021) Genes involved in mRNA surveillance are induced in *Brachypodium distachyon* under cadmium toxicity. Mol Biol Rep 49:5303–5313. https://doi.org/10.1007/s11033-021-06952-3.

Alves LR, Prado ER, de Oliveira R, Santos EF, Lemos de Souza I, Dos Reis AR, Azevedo RA, Gratao PL (2020) Mechanisms of cadmium-stress avoidance by selenium in tomato plants. Ecotoxicology 29:594–606.

Arrivault S, Senger T, Kramer U (2006) The Arabidopsis metal tolerance protein AtMTP3 maintains metal homeostasis by mediating Zn exclusion from the shoot under Fe deficiency and Zn oversupply. Plant J 46:861–879.

Barber-Zucker S, Shaanan B, Zarivach R (2017) Transition metal binding selectivity in proteins and its correlation with the phylogenomic classification of the cation diffusion facilitator protein family. Sci Rep 7:16381.

Chauhan DK, Yadav V, Vaculik M et al. (2021) Aluminum toxicity and aluminum stress-induced physiological tolerance responses in higher plants. Crit Rev Biotechnol 41:715–730.

Cheng J, Wang X, Liu X et al. (2021) Chromosome-level genome of Himalayan yew provides insights into the origin and evolution of the paclitaxel biosynthetic pathway. Mol Plant 14:1199–1209.

Chunna Y, Hong G, Yangyang Z et al. (2017) Identification of potential genes that contributed to the variation in the taxoid contents between two *Taxus* species (*Taxus media* and *Taxus mairei*). Tree Physiol 37:1659–1671.

Clemens S (2006) Toxic metal accumulation, responses to exposure and mechanisms of tolerance in plants. Biochimie 88: 1707–1719.

Clemens S, Aarts MG, Thomine S, Verbruggen N (2013) Plant science: the key to preventing slow cadmium poisoning. Trends Plant Sci 18:92–99.

Considine MJ, Foyer CH (2021) Stress effects on the reactive oxygen species-dependent regulation of plant growth and development. J Exp Bot 72:5795–5806.

Delhaize E, Gruber BD, Pittman JK, White RG, Leung H, Miao Y, Jiang L, Ryan PR, Richardson AE (2007) A role for the AtMTP11 gene of Arabidopsis in manganese transport and tolerance. Plant J 51:198–210.

Eroglu S, Giehl RFH, Meier B et al. (2017) Metal tolerance protein 8 mediates manganese homeostasis and iron reallocation during seed development and germination. Plant Physiol 174:1633–1647.

Gao Y, Yang F, Liu J, Xie W, Zhang L, Chen Z, Peng Z, Ou Y, Yao Y (2020) Genome-wide identification of metal tolerance protein genes in *Populus trichocarpa* and their roles in response to various heavy metal stresses. Int J Mol Sci 21:1680.

Grabherr MG, Haas BJ, Yassour M et al. (2011) Full-length transcriptome assembly from RNA-Seq data without a reference genome. Nat Biotechnol 29:644–652.

Gronberg C, Hu Q, Mahato DR et al. (2021) Structure and ion-release mechanism of PIB-4-type ATPases. Elife 10:e73124.

Gu D, Zhou X, Ma Y, Xu E, Yu Y, Liu Y, Chen X, Zhang W (2021) Expression of a *Brassica napus* metal transport protein (BnMTP3) in *Arabidopsis thaliana* confers tolerance to Zn and Mn. Plant Sci 304:110754.

Gueldry O, Lazard M, Delort F, Dauplais M, Grigoras I, Blanquet S, Plateau P (2003) Ycf1p-dependent hg(II) detoxification in *Saccharomyces cerevisiae*. Eur J Biochem 270:2486–2496.

Guo Z, Yuan X, Li L, Zeng M, Yang J, Tang H, Duan C (2022) Genome-wide analysis of the ATP-binding cassette (ABC) transporter family in *Zea mays* L. and its response to heavy metal stresses. Int J Mol Sci 23:2109.

Gustin JL, Zanis MJ, Salt DE (2011) Structure and evolution of the plant cation diffusion facilitator family of ion transporters. BMC Evol Biol 11:76.

Haddad R, Alrabadi N, Altaani B, Li T (2022) Paclitaxel drug delivery systems: focus on nanocrystals' surface modifications. Polymers (Basel) 14:658.

Han PP, Zhou J, Yuan YJ (2009) Analysis of phospholipids, sterols, and fatty acids in *Taxus chinensis* var. *mairei* cells in response to shear stress. Biotechnol Appl Biochem 54:105–112.

Haque A, Rahman MA, Das U, Rahman MM, Elseehy MM, El-Shehawi AM, Parvez MS, Kabir AH (2022) Changes in physiological responses and MTP (metal tolerance protein) transcripts in soybean (*Glycine max*) exposed to differential iron availability. Plant Physiol Biochem 179:1–9.

Heppel SC, Jaffe FW, Takos AM, Schellmann S, Rausch T, Walker AR, Bogs J (2013) Identification of key amino acids for the evolution of promoter target specificity of anthocyanin and proanthocyanidin regulating MYB factors. Plant Mol Biol 82:457–471.

Hu WJ, Liu TW, Zhu CQ et al. (2022) Physiological, proteomic analysis, and calcium-related gene expression reveal *Taxus wallichiana* var. *mairei* adaptability to acid rain stress under various calcium levels. Front Plant Sci 13:845107.

Ibuot A, Dean AP, Pittman JK (2020) Multi-genomic analysis of the cation diffusion facilitator transporters from algae. Metallomics 12:617–630.

Ismael MA, Elyamine AM, Moussa MG, Cai M, Zhao X, Hu C (2019) Cadmium in plants: uptake, toxicity, and its interactions with selenium fertilizers. Metallomics 11:255–277.

Jiao J, Xu XJ, Lu Y, Liu J, Fu YJ, Fu JX, Gai QY (2022) Identification of genes associated with biosynthesis of bioactive flavonoids and taxoids in *Taxus cuspidata* Sieb. et Zucc. Plantlets exposed to UV-B radiation. Gene 823:146384.

Kaur R, Das S, Bansal S, Singh G, Sardar S, Dhar H, Ram H (2021) Heavy metal stress in rice: uptake, transport, signaling, and tolerance mechanisms. Physiol Plant 173:430–448.

Kohli SK, Khanna K, Bhardwaj R, Abd Allah EF, Ahmad P, Corpas FJ (2019) Assessment of subcellular ROS and NO metabolism in higher plants: multifunctional signaling molecules. Antioxidants (Basel) 8:641.

Li D, He G, Tian W, Saleem M, Huang Y, Meng L, Wu D, He T (2021) Comparative and systematic omics revealed low cd accumulation of potato StMTP9 in yeast: suggesting a new mechanism for heavy metal detoxification. Int J Mol Sci 22:10478.

Li ZS, Lu YP, Zhen RG, Szczypka M, Thiele DJ, Rea PA (1997) A new pathway for vacuolar cadmium sequestration in *Saccharomyces cerevisiae*: YCF1-catalyzed transport of bis(glutathionato)cadmium. Proc Natl Acad Sci USA 94:42–47.

Liu X, Yu W, Zhang X, Wang G, Cao F, Cheng H (2017) Identification and expression analysis under abiotic stress of the R2R3-MYB genes in *Ginkgo biloba* L. Physiol Mol Biol Plants 23:503–516.

Ma G, Li J, Li J, Li Y, Gu D, Chen C, Cui J, Chen X, Zhang W (2018) OsMTP11, a trans-Golgi network localized transporter, is involved in manganese tolerance in rice. Plant Sci 274:59–69.

Meng D, Yu X, Ma L et al. (2017) Transcriptomic response of Chinese yew (*Taxus chinensis*) to cold stress. Front Plant Sci 8:468.

Menguer PK, Farthing E, Peaston KA, Ricachenevsky FK, Fett JP, Williams LE (2013) Functional analysis of the rice vacuolar zinc transporter OsMTP1. J Exp Bot 64:2871–2883.

Migocka M, Maciaszczyk-Dziubinska E, Malas K, Posyniak E, Garbiec A (2019) Metal tolerance protein MTP6 affects mitochondrial iron and manganese homeostasis in cucumber. J Exp Bot 70: 285–300.

Migocka M, Papierniak A, Kosieradzka A, Posyniak E, Maciaszczyk-Dziubinska E, Biskup R, Garbiec A, Marchewka T (2015) Cucumber metal tolerance protein CsMTP9 is a plasma membrane H(+)-coupled antiporter involved in the Mn(2)(+) and cd(2)(+) efflux from root cells. Plant J 84:1045–1058.

Migocka M, Malas K, Maciaszczyk-Dziubinska E, Papierniak A, Posyniak E, Garbiec A (2018) Cucumber metal tolerance protein 7 (CsMTP7) is involved in the accumulation of Fe in mitochondria under Fe excess. Plant J 95:988–1003.

Montanini B, Blaudez D, Jeandroz S, Sanders D, Chalot M (2007) Phylogenetic and functional analysis of the cation diffusion facilitator (CDF) family: improved signature and prediction of substrate specificity. BMC Genomics 8:107.

Moulis JM (2010) Cellular mechanisms of cadmium toxicity related to the homeostasis of essential metals. Biometals 23:877–896.

Najeeb U, Jilani G, Ali S, Sarwar M, Xu L, Zhou W (2011) Insights into cadmium induced physiological and ultra-structural disorders in *Juncus effusus* L. and its remediation through exogenous citric acid. J Hazard Mater 186:565–574.

Papierniak-Wygladala A, Kozak K, Barabasz A, Palusinska M, Calka M, Maslinska K, Antosiewicz DM (2020) Identification and characterization of a tobacco metal tolerance protein, NtMTP2. Metallomics 12:2049–2064.

Salinitro M, Mattarello G, Guardigli G, Odajiu M, Tassoni A (2021) Induction of hormesis in plants by urban trace metal pollution. Sci Rep 11:20329.

Sharma SS, Dietz KJ (2009) The relationship between metal toxicity and cellular redox imbalance. Trends Plant Sci 14:43–50.

Shingu Y, Kudo T, Ohsato S, Kimura M, Ono Y, Yamaguchi I, Hamamoto H (2005) Characterization of genes encoding metal tolerance proteins isolated from *Nicotiana glauca* and *Nicotiana tabacum*. Biochem Biophys Res Commun 331:675–680.

Singh S, Parihar P, Singh R, Singh VP, Prasad SM (2015) Heavy metal tolerance in plants: role of transcriptomics, proteomics, metabolomics, and ionomics. Front Plant Sci 6:1143.

Song C, Fu F, Yang L et al. (2021) *Taxus yunnanensis* genome offers insights into gymnosperm phylogeny and taxol production. Commun Biol 4:1203.

Su T, Fu L, Kuang L, Chen D, Zhang G, Shen Q, Wu D (2022) Transcriptome-wide m6A methylation profile reveals regulatory networks in roots of barley under cadmium stress. J Hazard Mater 423:127140.

Xiong X, Gou J, Liao Q et al. (2021) The Taxus genome provides insights into paclitaxel biosynthesis. Nat Plants 7:1026–1036.

Yang F, Gao Y, Liu J, Chen Z, de Dios VR, Gao Q, Zhang M, Peng Z, Yao Y (2021) Metal tolerance protein MTP6 is involved in Mn and co distribution in poplar. Ecotoxicol Environ Saf 226:112868.

Ye J, Zhang Y, Cui H et al. (2018) WEGO 2.0: a web tool for analyzing and plotting GO annotations, 2018 update. Nucleic Acids Res 46:W71–W75.

Yu C, Guo H, Zhang Y et al. (2017) Identification of potential genes that contributed to the variation in the taxoid contents between two Taxus species (*Taxus media* and *Taxus mairei*). Tree Physiol 37:1659–1671.

Yu C, Luo X, Zhang C et al. (2020) Tissue-specific study across the stem of *Taxus media* identifies a phloem-specific TmMYB3 involved in the transcriptional regulation of paclitaxel biosynthesis. Plant J 103:95–110.

Yu C, Zhang C, Xu X, Huang J, Chen Y, Luo X, Wang H, Shen C (2021) Omic analysis of the endangered Taxaceae species *Pseudotaxus chienii* revealed the differences in taxol biosynthesis pathway between *Pseudotaxus* and *Taxus yunnanensis* trees. BMC Plant Biol 21: 104.

Yu C, Huang J, Wu Q et al. (2022) Role of female predominant MYB39-bHLH13 complex in sexually dimorphic accumulation of taxol in *Taxus media*. Hortic Res 9:uhac062. https://doi.org/10.1093/hr/uhac062.

Yu H, Chen Z, Shang H, Cao J (2017) Physiological and biochemical responses of *Machilus ichangensis* Rehd. et Wils and *Taxus chinensis* (Pilger) Rehd. to elevated O_3 in subtropical China. Environ Sci Pollut Res Int 24:17418–17427.

Zhang F, Xiao X, Wu X (2020) Physiological and molecular mechanism of cadmium (Cd) tolerance at initial growth stage in rapeseed (*Brassica napus* L.). Ecotoxicol Environ Saf 197:110613.

Zhang M, Liu B (2017) Identification of a rice metal tolerance protein OsMTP11 as a manganese transporter. PloS One 12:e0174987.

Zhang P, Wang R, Ju Q, Li W, Tran LP, Xu J (2019) The R2R3-MYB transcription factor MYB49 regulates cadmium accumulation. Plant Physiol 180:529–542.

Zheng W, Komatsu S, Zhu W, Zhang L, Li X, Cui L, Tian J (2016) Response and defense mechanisms of *Taxus chinensis* leaves under UV-A radiation are revealed using comparative proteomics and metabolomics analyses. Plant Cell Physiol 57:1839–1853.

Zhu S, Shi W, Jie Y, Zhou Q, Song C (2020) A MYB transcription factor, BnMYB2, cloned from ramie (*Boehmeria nivea*) is involved in cadmium tolerance and accumulation. PloS One 15:e0233375.

Zou T, Lin R, Pu L, Mei Q, Wang Z, Jian S, Zhang M (2021) Genome-wide identification, structure characterization, expression pattern profiling, and substrate specificity of the metal tolerance protein family in *Canavalia rosea* (Sw.) DC. Plants (Basel) 10:1340. https://doi.org/10.3390/plants10071340.

Zu YG, Pang HH, Yu JH, Li DW, Wei XX, Gao YX, Tong L (2010) Responses in the morphology, physiology and biochemistry of *Taxus chinensis* var. *mairei* grown under supplementary UV-B radiation. J Photochem Photobiol B 98:152–158.